


RESEARCH ARTICLE OPEN ACCESS

Association Between Single Nucleotide Polymorphisms in the Aquaporin-4 Gene and Longitudinal Changes in White Matter Free Water and Cognitive Function in Non-Demented Older Adults

Lingyun Liu^{1,2} | Qingze Zeng² | Xiao Luo² | Hui Hong² | Yi Fang³ | Linyun Xie² | Yao Zhang² | Miao Lin² | Shuyue Wang² | Kaicheng Li² | Xiaocao Liu² | Ruiting Zhang² | Yanxing Chen³  | Yunjun Yang¹ | Peiyu Huang^{1,2} 

¹Department of Radiology, The First Affiliated Hospital of Wenzhou Medical University, Wenzhou, China | ²Department of Radiology, The Second Affiliated Hospital of Zhejiang University School of Medicine, Hangzhou, China | ³Department of Neurology, The Second Affiliated Hospital of Zhejiang University School of Medicine, Hangzhou, China

Correspondence: Yunjun Yang (yyjunjim@163.com) | Peiyu Huang (huangpy@zju.edu.cn)

Received: 24 November 2024 | **Revised:** 19 January 2025 | **Accepted:** 11 February 2025

Funding: This work was supported by Natural Science Foundation of Zhejiang Province, LZ24H180002, National Natural Science Foundation of China, 82371907, 82101987, 82202090, 82271936, 82371190.

Keywords: Alzheimer's disease | aquaporin-4 | glymphatic system | magnetic resonance imaging | single-nucleotide polymorphisms

ABSTRACT

We investigated whether aquaporin-4 (AQP4) single-nucleotide polymorphisms (SNPs) influence Alzheimer's disease (AD) progression through changes in the glymphatic system. We included 242 non-dementia participants and chose six SNPs previously shown to be related to AD. We analyzed the associations between AQP4 SNPs and glymphatic markers, including enlarged perivascular spaces (PVS), white matter free water (FW), and diffusion tensor image analysis along the perivascular space (DTI-ALPS), in both cross-sectional and longitudinal data. We investigated whether AQP4-related glymphatic markers are associated with AD pathology progression and cognitive impairment, and whether they mediate the relationship between AQP4 SNPs and AD progression. There was no association between AQP4 SNPs and glymphatic markers at baseline. Carriers of the AQP4 SNP rs72878794 minor allele status exhibited slower FW increase in the amyloid-positive group (SNP*time: $\beta = -0.0040$, $t(46.25) = -2.062$, $p = 0.045$, 95% CI = $-0.0078 \sim -0.0001$), whereas the rs9951307 minor allele carrier showed a faster FW increase in the amyloid-negative group (SNP*time: $\beta = 0.0033$, $t(81.19) = 2.245$, $p = 0.027$, 95% CI = $0.0004 \sim 0.0062$). The higher FW was associated with faster cognitive decline at follow-ups. AQP4 SNPs influence interstitial fluid accumulation, contributing to cognitive decline but not amyloid deposition in AD. Further studies are needed to clarify the pathways linking AQP4 SNPs and AD progression.

Abbreviations: AD, Alzheimer's disease; APOE, Apolipoprotein; AQP4, Aquaporin-4; A β , Amyloid-beta; BG, Basal ganglia; CDR, Clinical Dementia Rating; CSF, Cerebrospinal fluid; CU, Cognitively unimpaired; DCE-MRI, Dynamic contrast-enhanced magnetic resonance imaging; DTI, Diffusion tensor image; DTI-ALPS, Diffusion tensor imaging analysis along the perivascular space; FW, Free water; ISF, Interstitial fluid; MCI, Cognitive impairment; MMSE, Mini-Mental State Examination; MoCA, Montreal Cognitive Assessment; MRI, Magnetic resonance imaging; PVS, Perivascular spaces; SNP, Single-nucleotide polymorphisms; TMT-A, Trial-Making Test-A; TMT-B, Trial-Making Test-B.

Lingyun Liu and Qingze Zeng contributed equally to this work.

This is an open access article under the terms of the [Creative Commons Attribution-NonCommercial](https://creativecommons.org/licenses/by-nc/4.0/) License, which permits use, distribution and reproduction in any medium, provided the original work is properly cited and is not used for commercial purposes.

© 2025 The Author(s). *Human Brain Mapping* published by Wiley Periodicals LLC.

1 | Background

The glymphatic system has been described as a “garbage truck” of the human brain (Nedergaard 2013). Studies demonstrated that cerebrospinal fluid (CSF) can flow into the perivascular spaces (PVS) surrounding penetrating arteries and enter the brain interstitial space through aquaporin-4 (AQP4) water channels located on the endfeet of astroglial cells, where CSF and interstitial fluid (ISF) mix and efflux, taking away brain metabolic wastes (Benveniste et al. 2017; Iliff et al. 2012; Nedergaard and Goldman 2020). Impairment of the glymphatic system may lead to the accumulation of pathological proteins, such as amyloid-beta ($A\beta$) and tau (Tiwari et al. 2019), the core pathologies of Alzheimer's disease (AD) (Keshavan et al. 2021), and contribute to the development of various neurological disorders (Fang et al. 2022; Vittorini et al. 2024).

Along the glymphatic pathway, the AQP4 channels are a crucial component (Mestre et al. 2018). They form abundant pores in the cell membrane, creating a high permeability that is essential for the rapid CSF–ISF exchange and waste clearance (Rasmussen et al. 2018; Zeppenfeld et al. 2017). Utilized brain autopsy data from non-AD and AD patients and found that the loss of perivascular AQP4 localization was associated with an increased amyloid burden. Through stereotactic injection of HiLyte 555 Tau into the brain of AQP4 KO mice, Ishida et al. (Ishida et al. 2022) found that tau was cleared from the brain to the CSF by an AQP4-dependent mechanism. Interestingly, single-nucleotide polymorphisms (SNPs) in the AQP4 gene may alter the functionality of AQP4 proteins and influence glymphatic function. Several recent studies found that variations in the AQP4 gene might accelerate $A\beta$ deposition and cognitive decline in humans (Burfeind et al. 2017; Chandra et al. 2021; Rainey-Smith et al. 2018). Nonetheless, there is a lack of human studies validating whether an altered glymphatic function mediates the association between gene variations and AD progression. Because AQP4 is also related to many other water exchange processes and degeneration mechanisms (Saadoun et al. 2005; Verkman 2012), clarifying the role of glymphatic clearance is necessary.

Currently, a few non-invasive magnetic resonance imaging (MRI) markers are considered to be related to glymphatic alterations. First, dilation of PVS, the main conduit of glymphatic flow, has been found to be associated with aging, hypertension, $A\beta$, and a variety of neurodegenerative disorders (Zeng et al. 2022). The dilation was considered a compensatory restructuring of PVS in response to reduced glymphatic flow (Brown et al. 2018). Second, interstitial water content assessed by free water (FW) imaging may reflect fluid stagnation due to glymphatic dysfunction. A previous study (Gomolka et al. 2023) found increased parenchymal water diffusivity in mice with AQP4 water channel deletion, supporting the association between parenchymal water content measured by MRI and glymphatic dysfunction. Third, diffusion tensor image analysis along the perivascular space (DTI-ALPS) (Taoka et al. 2017), an index measuring fluid transport in the perivenous space along the deep medullary veins, has demonstrated a good association with glymphatic clearance measured by DCE-MRI (Zhang, Huang, et al. 2021; Zhang, Zhou, et al. 2021). While there are still debates regarding whether they could reflect global glymphatic function, these markers have been chosen due to the paucity of available MRI markers. Several previous studies

have demonstrated their close association with clinical status and pathological deposition (Hong et al. 2024; Kamagata et al. 2022; Perosa et al. 2022).

In the present study, we aim to study whether AQP4 SNPs are associated with glymphatic function and clinical progression in non-demented older adults. Specifically, we aim to study (1) the association between AQP4 SNPs and glymphatic markers through both cross-sectional and longitudinal analyses and (2) whether changes in glymphatic markers mediate the association between AQP4 SNPs and AD progression.

2 | Materials and Methods

All procedures conducted in studies involving human participants adhered to the ethical standards set forth by the Institutional and National Research Committees, as well as the 1964 Declaration of Helsinki and its subsequent amendments or equivalent ethical guidelines. Written informed consent was obtained from all participants, their authorized representatives, and study partners prior to the initiation of any protocol-specific procedures in the ADNI study. All data were downloaded at September 2023 from ADNI 2 & 3. Further information is available at <http://www.adni-info.org>.

2.1 | Study Participants

The inclusion criteria included (1) non-demented participants, including cognitively unimpaired participants (CU, $N=126$) and mild cognitive impairment participants (MCI, $N=116$). The diagnoses were made by neurologists at admission. The CUs were defined as subjects who had a Clinical Dementia Rating (CDR) scale score of 0, a Mini-Mental State Examination (MMSE) between 24 and 30 (inclusive), Wechsler memory scale logical memory (WMS-LM) delay recall performance ≥ 9 for subjects with 16 or more years of education; ≥ 5 for subjects with 8–15 years of education; and ≥ 3 for 0–7 years of education; non-clinical depression (GDS-15 score < 6), and absence of dementia. MCI was defined as subjects who had preserved activities of daily living, non-dementia, and objective cognitive impairments, as shown on the delayed recall test of the WMS-LM, as well as a CDR score of 0.5(2) with available T1-weighted structural images, diffusion tensor imaging (DTI) images, and $A\beta$ PET data; (3) with gene sequencing information; and (4) with neuropsychological assessments. Exclusion criteria were as follows (Li et al. 2023): (1) significant medical, neurological, and psychiatric illness, (2) head trauma history, (3) use of non-AD-related medication known to influence cerebral function, and (4) alcohol or drug abuse.

To ensure the maximum sample size, for participants with multiple follow-up timepoints, we considered the first timepoint that met all inclusion criteria as the baseline timepoint. Available follow-up data (varied from 0 to 10.25 years) were also collected (see flowchart in Figure 1).

Vascular risk factor score (VRFs), including hypertension, diabetes, hyperlipidemia, and smoking, was recorded based on participants' medical history. Each factor was coded as 0 (absent) or 1 (present), resulting in a total score ranging from 0 to 4.

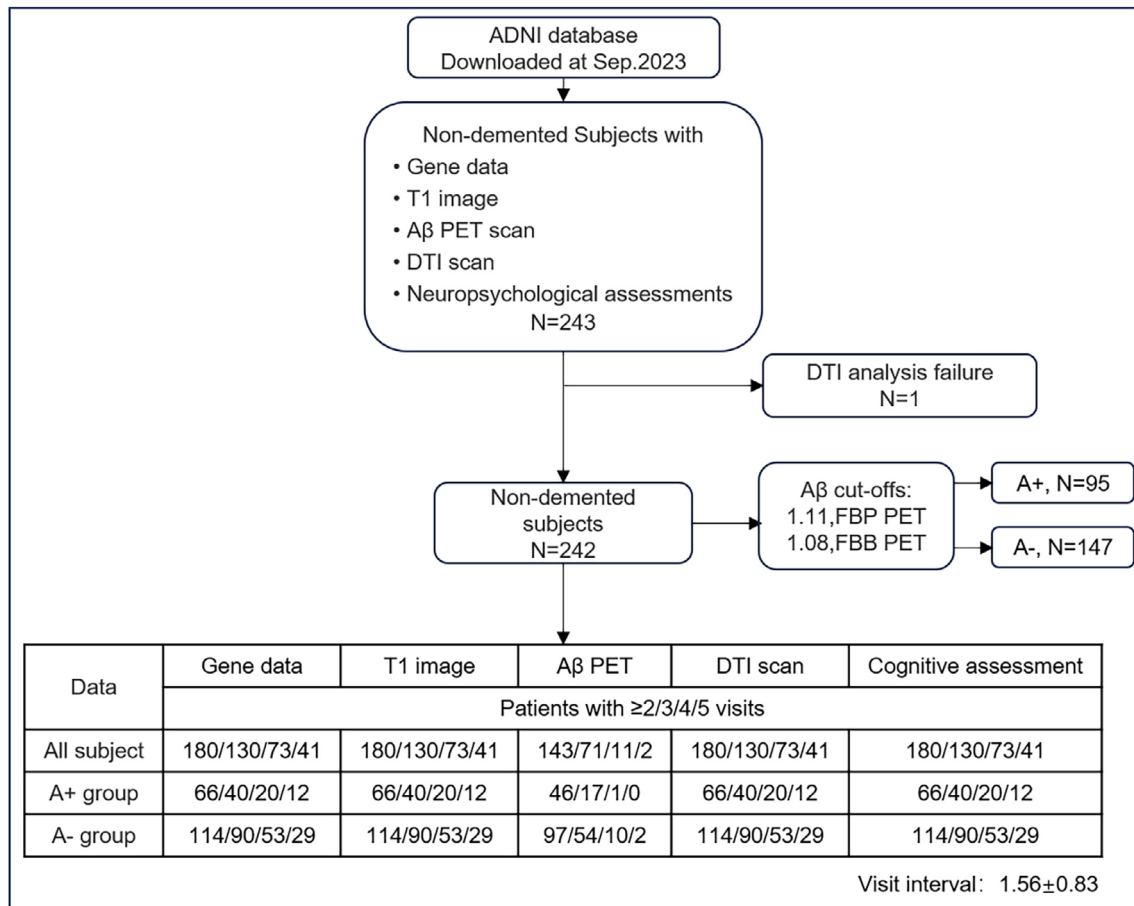


FIGURE 1 | Flowchart of the subject inclusion: 242 non-demented participants were included for analyses, listing the number of subjects with 2, 3, 4, or 5 visits for each modality. For the cutoffs of brain amyloid, participants were categorized as Aβ positive (A+) and Aβ negative (A-). ADNI, Alzheimer's disease neuroimaging initiative; DTI, diffusion tensor imaging; FBB, [18F] florbetaben; FBP, [18F] florbetapir; PET, positron emission tomography.

2.2 | Neuropsychological Assessment

Primary measures were global cognitive function, episodic memory, and executive function. Global cognition assessments (Oh et al. 2021) included the MMSE, Montreal Cognitive Assessment (MoCA), and CDR (Tsang et al. 2015). Logical Memory-Delayed Recall (Tedeschi Dauar et al. 2023) was used to assess episodic memory. The Trails Making Test Part A and Part B (TMT-A and TMT-B) (Dikmen et al. 1999) were used to assess executive function.

2.3 | Genetic Analysis

Participants carrying at least one apolipoprotein (APOE) ε4 allele were classified as carriers, while the rest were categorized as noncarriers. Whole-genome sequencing data were downloaded from the ADNI database. To store statistically relevant SNPs called using Illumina's CASAVA SNP Caller, the ADNI WGSSNP data are stored in variant call format (VCF). SNP pruning was undertaken using PLINK (Purcell et al. 2007). Genetic variants of AQP4 underwent quality control procedures. Specifically, we removed the SNPs that were not in Hardy-Weinberg equilibrium ($p < 0.05$) (Hosking et al. 2004) and had a minor allele frequency of $< 5\%$ (Tabangin et al. 2009). Linkage disequilibrium-based

SNP pruning (Hill and Robertson 1968) was performed to reduce statistical redundancy and maintain coverage of the AQP4 gene. From the rest of the SNPs, six SNPs that had been shown to be clinically relevant in AD were chosen. The results are shown in Figure S1. The information on these SNPs is displayed in Table 1 and Figure 2. Participants possessing one or two copies of the minor allele were classified as "carriers" for the SNP. Details were provided in the Supporting Information.

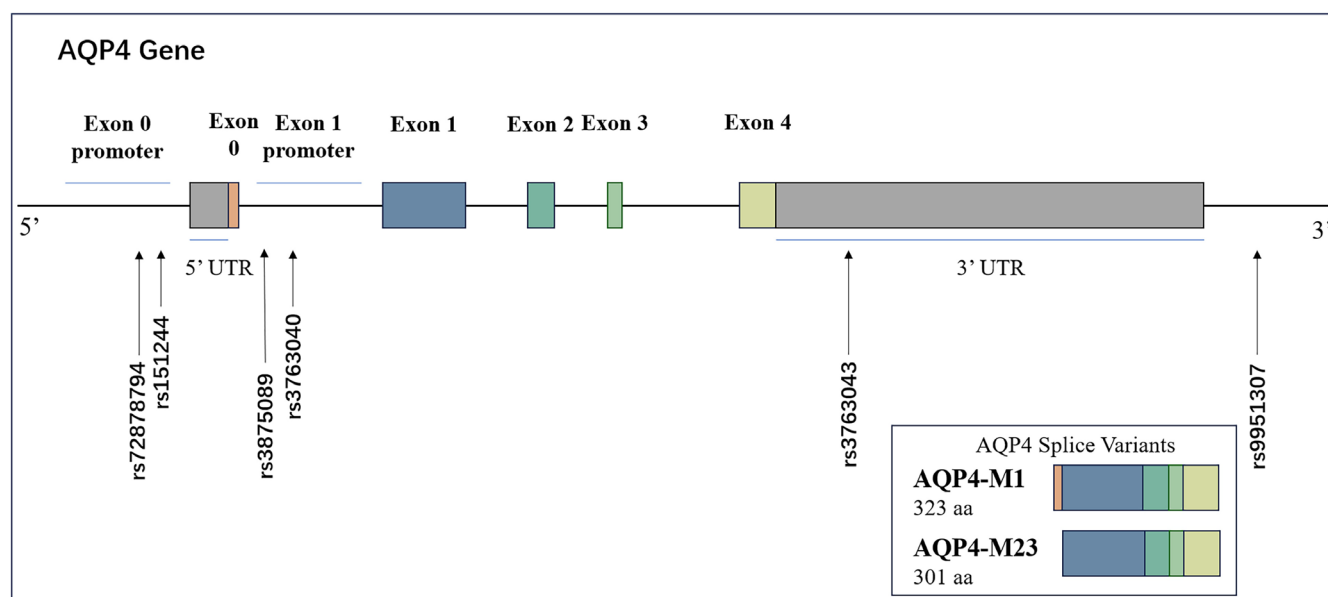
2.4 | Imaging Acquisition

The ADNI imaging data were acquired from different centers using harmonized protocols, and the full list of acquisition parameters can be seen on the ADNI website (<https://adni.loni.usc.edu/methods/documents/mri-protocols/>). All imaging data were acquired using 3T scanners from three vendors (GE, Siemens, and Philips). Here, we list some representative imaging parameters:

The structural images were obtained based on a 3D Spoiled Gradient Recalled Echo T1 weighted sequence, with the following parameters: Flip Angle = 11° ; Matrix X = 256 pixels; Matrix Y = 256 pixels; voxel size = $1 \times 1 \times 1.2 \text{ mm}^3$; echo time (TE) = minimum; inversion time (TI) = 400 msec; repetition time (TR) = 7.34 msec; 196 sagittal slices. The axial

TABLE 1 | AQP4 SNPs included in this study.

	Annotation	Position (GRCh38)	Minor allele frequency	Previously reported associations
rs9951307 G/A	downstream	chr18:26850565	0.172	Cognitive decline in AD (Burfeind et al. 2017)
rs3763043 C/T	3'-UTR	chr18:26855854	0.318	Cognitive decline in AD (Burfeind et al. 2017)
rs3763040 G/A	Exon 1 promoter	chr18:26864410	0.192	Cognitive decline in AD (Burfeind et al. 2017)
rs3875089 T/C	Exon 1 promoter	chr18:26865469	0.149	Cognitive decline in AD (Burfeind et al. 2017)
rs151244 T/C	Exon 0 promoter	chr18:26866755	0.294	Cognitive decline in AD (Chandra et al. 2021)
rs72878794 C/T	Exon 0 promoter	chr18:26866839	0.038	Cognitive decline in AD (Chandra et al. 2021)

**FIGURE 2** | Schematic illustration of the investigated SNPs in the AQP4 gene. There are two isoforms of AQP4: M1 and M23. M1 consists of exon 0–4, and M23 consists of exon 1–4.

T2 FLAIR sequence used the following parameters: Flip Angle = 90.0/125.0°; Matrix $X=256$ pixels; Matrix $Y=256$ pixels; voxel size = $0.9 \times 0.9 \times 5.0$ mm³; TE = 147.9–154.0 msec; TI = 2250.0 msec; TR = 11000.0 msec. DTI images were obtained with a Spin Echo Sequence using the following imaging parameters: $b=0/1000$ s/mm², non-diffusion-weighted image = 5, 41 MPG axes, TR = 9050 msec, TE = 63.0 msec, flip angle of 90°, 1.37 mm \times 1.37 mm voxel, 2.70 slice thickness, and 46 axial slices.

The amyloid PET was performed using two tracers, including florbetapir or florbetaben. The detailed acquisition procedures were described in the ADNI PET Technical Procedures Manual (http://adni.loni.usc.edu/wp-content/uploads/2010/05/ADNI2_PET_Tech_Manual_0142011.pdf). For the cutoffs of brain amyloid, the values were 1.11 for 18F-florbetapir (18[F]-AV45) SUVR and 1.08 for 18F-florbetaben (FBB) SUVR (Royse et al. 2021);

according to the cutoff, participants were categorized as A β positive (A+) and A β negative (A–). For continuous brain amyloid SUVR, cortical amyloid SUVRs obtained from different PET tracers were harmonized by UC Berkeley and Lawrence Berkeley National Laboratory. These SUVRs were normalized using the whole cerebellum and then transformed into Centiloids.

2.5 | Imaging Analysis

2.5.1 | PVS Visual Rating

PVS in the basal ganglia (BG) and white matter (WM) region were assessed on T1-weighted images by two postgraduate students (LX; LL) according to a previously proposed rating scale (Zhu et al. 2011). Briefly, in the BG region, PVS was rated 1: < 5 enlarged PVS (ePVS), rated 2: 5–10 ePVS, rated

3: > 10 ePVS but the number is still countable, and rated 4: uncountable; in the WM region, PVS severity was rated 1: < 10 ePVS in total, rated 2: > 10 PVS in total but no more than 10 ePVS in a single section, rated 3: 10–20 ePVS in the section containing the greatest number of ePVS, and rated 4: > 20 ePVS in any single section.

2.5.2 | DTI-ALPS Calculation

The processing of DTI data was conducted using FSL 6.0 (<https://fsl.fmrib.ox.ac.uk/fsl>). The preprocessing steps included skull stripping, denoising, removing Gibbs artifact, EPI distortion correction, and eddy current correction.

DTI-ALPS was calculated referring to the previous article (Taoka et al. 2017). Briefly, the FA maps and diffusivity maps [Dxx, Dyy, Dzz] were acquired from preprocessed diffusion data using dtifit and then co-registered to the MNI space through b0 images. Four cross-regions of interest (ROIs) containing five voxels (40 mm³) were manually placed in the areas of bilateral projection fiber (proj) and association fiber. The left and right ALPS index was calculated as [(Dxx-proj + Dxx-assoc) / (Dyy-proj + Dzz-assoc)] on each side, respectively. The mean ALPS index is defined by the average of bilateral ALPS indexes.

2.5.3 | FW Calculation

The FW map was calculated using the script from the MarkVCID (<https://markvcid.partners.org/>). The MarkVCID is a consortium of US academic medical centers. Its mission is to identify and validate biomarkers for the small vessel diseases of the brain that produce vascular contributions to cognitive impairment and dementia. FW was estimated using a two-compartment model (Pasternak et al. 2009) by fitting the diffusion data of water molecules to two tensors. First, the extracellular FW was quantified to obtain the isotropic FW compartment and the FW volume fraction. Second, after removing the influence of FW, the anisotropic tissue compartment was obtained through the second DTI modeling to obtain the DTI index after the correction of FW separation. The FW map represents the fractional volume in every voxel (ranging from 0 to 1) of the FW compartment. Finally, the generated FW maps were registered to structural images through b0 images, and the mean FW in the WM was extracted.

2.5.4 | Statistical Analysis

All the statistical analyses were performed in R (version 4.3.0) and SPSS Statistics, Version 25.0 (IBM). Demographic characteristics between groups were compared using the *t*-test for normally distributed continuous variables, the Mann–Whitney U test for non-normally distributed continuous variables, and chi-square tests for categorical variables. To reduce site effects, we conducted multicenter data harmonization on diffusion metrics FW and DTI-ALPS using the COMBAT method with age and sex included as biological variables (Fortin et al. 2017).

To remove possible influences of WM microstructural properties on DTI-ALPS assessment (Huang et al. 2024), we also included the whole brain WM mean diffusivity (MD) as a covariate in the analyses involving the DTI-ALPS index. All analyses were performed in the whole group, the A+ group, and the A− group separately.

2.5.5 | Correlation Among the Three Imaging Markers

First, we tested the correlations among the three imaging markers. Pearson correlation was used to investigate the correlation between FW and DTI-ALPS, and Spearman's correlation was used to investigate the correlation between FW\DTI-ALPS and PVS scores.

2.5.6 | The Association Between AQP4 SNPS and Glymphatic Markers

For baseline cross-sectional analysis, multiple linear regression analysis was used to assess the associations between AQP4 SNPs and glymphatic markers, with age, sex, and VRFs as covariates.

Model1: glymphatic marker ~ SNP1 + ... + SNP6 + age + sex + VRFs.

For the association between AQP4 SNPs and longitudinal changes in each glymphatic marker, linear mixed models (lme4, R statistics) were employed, with AQP4 SNPs and their interactions with time as independent variables and each glymphatic marker as the dependent variable. Age, sex, and VRFs were introduced as covariates.

Model2: glymphatic marker ~ SNP1 × time + ... + SNP6 × time + SNP1 + ... + SNP6 + time + age + sex + VRFs + (1 + time | Subject).

2.5.7 | The Association Between the AQP4 SNP-Related Glymphatic Marker and Clinical Characteristics

For baseline cross-sectional analysis, multiple linear regression analysis was used to assess the associations between the AQP4 SNP-related glymphatic marker (i.e., FW) and amyloid accumulation and cognitive performance. When analyzing the association between FW and amyloid accumulation, age, sex, VRFs, and the status of APOE ε4 carriers were included as covariates. When analyzing the association between FW and cognitive performance, education was additionally added as a covariate. The equations for each model were as follows:

Model3: Amyloid PET Centiloids ~ FW + age + sex + VRFs + APOE ε4.

Model4: cognitive measure ~ FW + age + sex + VRFs + APOE ε4 + education.

Linear mixed models were also employed to investigate the association between baseline FW and changes in amyloid

accumulation and cognition. When analyzing the association between baseline FW and changes in amyloid accumulation, age, sex, VRFs, and APOE $\epsilon 4$ status were included as covariates. When analyzing the association between baseline FW and the changes in cognition, education was additionally included as a covariate.

Model5: Amyloid PET Centiloids \sim FW \times time + FW + time + age + sex + VRFs + APOE $\epsilon 4$ + (1 + time | Subject).

Model6: cognitive measure \sim FW \times time + FW + time + age + sex + VRFs + education + APOE $\epsilon 4$ + (1 + time | Subject).

2.5.8 | Mediation Analyses

After the previous steps, we found associations between the SNPs, FW, and cognitive measures. To test whether FW mediated the associations between SNPs and cognitive measures, we built several mediation models (Figures S2–S6). In the A β positive group: (1) SNP rs72878794 \rightarrow FW \rightarrow CDR ratio, (2) SNP rs72878794 \rightarrow FW \rightarrow Logical Memory-Delayed Recall score ratio, and (3) SNP rs72878794 \rightarrow FW \rightarrow TMT-A time ratio. In the A β negative group: (1) SNP rs9951307 \rightarrow FW \rightarrow CDR ratio, and (2) SNP rs9951307 \rightarrow FW \rightarrow TMT-A time ratio.

Specifically, we used linear mixed models to extract the annual change ratio of FW and cognitive measures and used the R “Mediation” package to build and analyze the mediation model. In all models, the AQP4 SNP was the independent variable, FW was the mediator, and the cognitive measure was the dependent variable. On the path SNP \rightarrow FW, we adjusted for age, sex, and VRFs; on the path SNP \rightarrow cognition, we adjusted for age, sex, VRFs, education, and APOE $\epsilon 4$ status. A 95% bootstrap confidence interval based on 10,000 bootstrap replicates was used to estimate significance.

The FDR correction method was used for multiple comparison corrections between glymphatic markers and cognitive scores at the level of three groups to control false positives. Considering the explorative nature of the current study, we reported all statistical results in the paper. The p-value for statistical significance was set at 0.05, two-tailed.

3 | Results

3.1 | Demographics

This study included 242 non-demented subjects, among which 95 subjects were A+, and 147 subjects were A–. Subjects in the A+ group had a higher age, more APOE $\epsilon 4$ variations, and higher amyloid PET Centiloids than the A– group. Subjects in the A+ group had significantly worse cognitive performances in MoCA, TMT-A, and TMT-B than the A– group. There were no significant differences in glymphatic markers between the A+ group and A– group; please see details in Table 2. Among the three imaging markers (Figure S10), BG-PVS was correlated with FW ($r = 0.190$, $p = 0.003$), and FW was correlated with DTI-ALPS ($r = -0.428$, $p < 0.001$).

3.2 | Associations Between AQP4 SNPs and the Glymphatic Imaging Markers

At baseline, none of the AQP4 SNPs was associated with glymphatic markers in the three groups. The detailed results are shown in Tables S1–S3.

For longitudinal analysis, PVS ratings were not included due to a high PVS burden at baseline. As shown in Table 2, both PVS rating scores in the BG and WM regions were high (3–4) in either the whole group, A+ group, or A– group, which introduced a ceiling effect and limited statistical power. Therefore, we only analyzed the changes in FW and ALPS.

As shown in Table 3, in the whole group, there was no association between AQP4 SNPs and FW changes. In the A+ group, the rs72878794 minor allele carrier status was associated with a slower increase in FW (SNP*time: $\beta = -0.0040$, $t(46.25) = -2.062$, $p = 0.045$, 95% CI = $-0.0078 \sim -0.0001$). In the A– group, we observed that the rs9951307 minor allele carrier status was associated with a faster increase in FW (SNP*time: $\beta = 0.0033$, $t(81.19) = 2.245$, $p = 0.027$, 95% CI = $0.0004 \sim 0.0062$). No significant associations had been found between the AQP4 SNPs and DTI-ALPs changes.

3.3 | Associations Between FW and Clinical Variables

In the cross-sectional analysis of the whole group (Table 4 and Figure S7), a higher FW was associated with a lower MMSE score (β -std = -0.162 , $t(232) = -2.207$, $p = 0.028$, 95% CI = $-0.307 \sim -0.017$), a lower MoCA score (β -std = -0.190 , $t(235) = -2.782$, $p = 0.006$, 95% CI = $-0.325 \sim -0.056$), a higher CDR score (β -std = 0.226 , $t(233) = 3.150$, $p = 0.002$, 95% CI = $0.084 \sim 0.367$), a lower Logical Memory-Delayed Recall score (β -std = -0.256 , $t(140) = -2.966$, $p = 0.004$, 95% CI = $-0.427 \sim -0.085$), and a longer TMT-B time (β -std = 0.223 , $t(234) = 3.282$, $p = 0.001$, 95% CI = $0.089 \sim 0.357$). For the A+ group (Table S5 and Figure S8), more details can be found in the Supporting Information. For the A– group (Table S6 and Figure S9), we observed associations between a higher FW and a lower MoCA score (β -std = -0.197 , $t(140) = -2.202$, $p = 0.029$, 95% CI = $-0.373 \sim -0.020$), a higher CDR score (β -std = 0.313 , $t(138) = 3.427$, $p = 0.001$, 95% CI = $0.133 \sim 0.494$), a lower Logical Memory-Delayed Recall score (β -std = -0.039 , $t(81) = -2.716$, $p = 0.008$, 95% CI = $-0.536 \sim -0.083$), and a longer TMT-B time (β -std = 0.255 , $t(139) = 2.974$, $p = 0.003$, 95% CI = $0.085 \sim 0.424$).

For longitudinal analysis in the whole group (Table 5), a higher baseline FW was associated with a faster decline in MMSE score (FW * time: $\beta = -2.952$, $t(119.06) = -3.425$, $p = 0.001$, 95% CI = $-4.679 \sim -1.239$), a faster increase in CDR score (FW * time: $\beta = 0.550$, $t(97.28) = 5.799$, $p < 0.001$, 95% CI = $0.361 \sim 0.737$), and a faster increase in TMT-A completion time (FW * time: $\beta = 20.491$, $t(245.26) = 4.543$, $p < 0.001$, 95% CI = $11.564 \sim 29.354$). In the A+ group (Table S7), a higher baseline FW was associated with a faster increase in CDR score (FW * time: $\beta = 0.675$, $t(36.68) = 4.087$, $p < 0.001$, 95% CI = $0.330 \sim 1.006$), a slower decline in Logical Memory-Delayed Recall score (FW * time: $\beta = 7.152$, $t(32.11) = 2.451$, $p = 0.020$, 95% CI = $1.256 \sim 13.066$),

TABLE 2 | Demographic data of participants at baseline.

	All (<i>n</i> = 242)	Group A+ (<i>n</i> = 95)	Group A– (<i>n</i> = 147)	<i>p</i>
Age(y)	76.69 ± 0.49	78.12 ± 7.18	75.77 ± 7.85	0.011
Female, <i>N</i> (%)	111 (45.9)	48 (50.5)	63 (42.9)	0.242
Education (y)	16.40 ± 0.17	16.03 ± 2.63	16.63 ± 2.72	0.057
Hypertension, <i>N</i> (%)	117 (48.3)	47 (49.5)	70 (47.6)	0.778
Hyperlipidemia, <i>N</i> (%)	85 (35.1)	33 (34.7)	52 (35.4)	0.919
Diabetes, <i>N</i> (%)	13 (5.4)	5 (5.3)	8 (5.4)	0.952
Smoking, <i>N</i> (%)	23 (9.5)	9 (9.5)	14 (9.5)	0.990
APOE ε4 carriers, <i>N</i> (%)	79 (32.6)	49 (51.6)	30 (20.4)	< 0.001
Amyloid PET Centiloids	25.52 ± 2.71	69.32 ± 34.50	−2.78 ± 10.11	< 0.001
Tau PET SUVR ^a	1.22 ± 0.01	1.26 ± 0.20	1.19 ± 0.11	0.186
Cognitive assessments				
MMSE	28.53 ± 0.10	28.33 ± 1.59	28.66 ± 1.38	0.142
MoCA	24.64 ± 0.21	23.97 ± 3.20	25.07 ± 3.25	0.003
CDR global	0.23 ± 0.02	0.30 ± 0.25	0.19 ± 0.24	0.001
Logical Memory-Delayed Recall	12.90 ± 0.42	12.03 ± 5.43	13.49 ± 4.71	0.178
TMT-A	34.90 ± 0.75	37.06 ± 11.52	33.50 ± 11.41	0.008
TMT-B	95.39 ± 3.64	106.15 ± 65.93	88.39 ± 48.47	0.039
Glymphatic markers				
Basal ganglia PVS	3 (3–3)	3 (3–3)	3 (3–3)	0.735
White matter PVS	4 (3–4)	4 (3–4)	4 (3–4)	0.906
FW	0.235 ± 0.003	0.242 ± 0.052	0.231 ± 0.041	0.107
DTI-ALPS ^b	1.290 ± 0.014	1.289 ± 0.212	1.290 ± 0.224	0.772

Note: Raw data were presented as mean (± standard deviation [SD]) or number (percentage, %) in tables unless otherwise noted. Data were compared using *t*-tests or chi-square tests.

Abbreviations: All, the whole group; A+, Aβ positive; A–, Aβ negative; DTI-ALPS, diffusion tensor image analysis along the perivascular space; FW, free water; MMSE, Mini-Mental State Exam; MoCA, Montreal Cognitive Assessment; PVS, perivascular space; TMT-A, Trail Making Test-A; TMT-B, Trail Making Test-B.

^aOf the whole group, 133 did not have tau information.

^bOne amyloid-negative participant without the DTI-ALPS index due to image registration failure.

and a faster increase in TMT-A completion time (FW * time: $\beta = 28.398$, $t(41.90) = 2.560$, $p = 0.014$, 95% CI = 6.255 ~ 50.780). In the A– group (Table S8), we also observed that higher baseline FW was associated with a faster increase in CDR score (FW * time: $\beta = 0.447$, $t(60.11) = 3.869$, $p < 0.001$, 95% CI = 0.218 ~ 0.679) and a faster increase in TMT-A completion time (FW * time: $\beta = 18.070$, $t(50.06) = 3.369$, $p = 0.001$, 95% CI = 6.962 ~ 28.750).

In both cross-sectional and longitudinal analyses, we did not observe any associations between FW and amyloid accumulation. The results are shown in Table S4.

3.4 | Mediation Analyses Between AQP4 SNPs, FW, and Cognitive Performance

In all models, we had not observed FW's mediation role between AQP4 SNPs and cognition. Specifically, in the Aβ positive

group, the effect of rs72878794 on CDR via FW was not significant ($\beta = -0.0047$, $p = 0.08$); the effect of rs72878794 on Logical Memory-Delayed Recall via FW was not significant ($\beta = 0.0246$, $p = 0.45$); the effect of rs72878794 on TMT-A via FW was not significant ($\beta = -0.1710$, $p = 0.34$). In the Aβ negative group, the effect of rs9951307 on the CDR ratio via FW was not significant ($\beta = -0.0005$, $p = 0.56$); the effect of rs9951307 on TMT-A ratio via FW was not significant ($\beta = 0.0557$, $p = 0.08$). Detailed results are shown in Figures S2–S6.

4 | Discussion

In this study, we explored the effects of AQP4 SNPs on glymphatic markers and AD progression in non-demented participants. Results showed that the AQP4 SNP rs72878794 minor allele carrier status was associated with a slower increase in FW in the Aβ positive group, and the AQP4 SNP rs9951307 minor

TABLE 3 | Associations between AQP4 SNPs and longitudinal glymphatic imaging markers change.

Independent variables	All group						A+ group						A− group					
	FW			DTI-ALPS			FW			DTI-ALPS			FW			DTI-ALPS		
	β	p		β	p		β	p		β	p		β	p		β	p	
Age	0.0031	<0.001		−0.0054	0.007		0.0029	<0.001		−0.0062	0.053		0.0030	<0.001		−0.0049	0.053	
Sex	−0.0023	0.698		−0.0797	0.002		0.0068	0.538		−0.0704	0.091		−0.0066	0.341		−0.0815	0.017	
VRFs	0.0036	0.284		0.0131	0.381		0.0055	0.377		−0.0308	0.194		0.0031	0.424		0.0389	0.043	
WM MD	—	—		−0.0660	<0.001		—	—		−0.0737	0.001		—	—		−0.0627	0.001	
Time	0.0036	0.002		−0.0135	0.068		0.0055	0.001		−0.0366	0.005		0.0029	0.063		−0.0047	0.603	
rs9951307	−0.0069	0.242		0.0049	0.869		−0.0087	0.423		−0.0384	0.424		−0.0053	0.449		0.0065	0.865	
rs3763043	−0.0106	0.076		−0.0233	0.432		−0.0245	0.030		−0.0412	0.412		−0.0033	0.639		−0.0123	0.744	
rs3763040	0.0032	0.602		−0.0129	0.675		0.0073	0.523		−0.0319	0.527		0.0023	0.761		0.0043	0.916	
rs3875089	−0.0023	0.733		−0.0013	0.970		0.0067	0.597		−0.0068	0.903		−0.0055	0.496		−0.0183	0.671	
rs151244	0.0062	0.298		−0.0340	0.251		0.0017	0.878		−0.0160	0.739		0.0061	0.405		−0.0543	0.170	
rs72878794	0.0086	0.259		−0.0229	0.548		0.0088	0.548		−0.0800	0.213		0.0051	0.567		0.0079	0.868	
rs9951307 × time	0.0018	0.110		−0.0071	0.286		−0.0016	0.305		0.0093	0.393		0.0033	0.027		−0.0123	0.142	
rs3763043 × time	−0.0007	0.559		0.0036	0.580		0.0022	0.198		0.0055	0.645		−0.0017	0.257		0.0013	0.872	
rs3763040 × time	−0.0020	0.093		0.0084	0.226		−0.0008	0.630		0.0191	0.096		−0.0027	0.088		0.0057	0.522	
rs3875089 × time	0.0004	0.779		−0.0052	0.486		−0.0017	0.360		0.0039	0.762		0.0012	0.474		−0.0078	0.394	
rs151244 × time	−0.0016	0.147		−0.0031	0.642		−0.0014	0.382		0.0010	0.933		−0.0014	0.374		−0.0057	0.508	
rs72878794 × time	−0.0007	0.586		0.0102	0.198		−0.0040	0.045		0.0097	0.464		0.0001	0.973		0.0106	0.275	

Note: Reported are estimates and p-values from linear mixed models with random intercepts and random slopes. The fixed effect of SNP*time was interpreted as the effect on longitudinal glymphatic change. Abbreviations: All, the whole group; A−, A β negative; A+, A β positive; DTI-ALPS, diffusion tensor image analysis along the perivascular space; FW, free water; MD, mean diffusivity; SNP, single-nucleotide polymorphism; VRFs, vascular risk factor score; WM, white matter.

TABLE 4 | Cross-sectional associations between glymphatic imaging markers and cognitive measures in the whole group.

Independent variables	Cognitive assessment									
	MMSE		MoCA		CDR global		Logistic delayed		TMT-A	
	β -std	p	β -std	p	β -std	p	β -std	p	β -std	p
Age	-0.008	0.920	-0.087	0.215	-0.141	0.056	0.062	0.515	0.217	0.003
Sex	0.011	0.876	0.162	0.010	-0.175	0.008	0.028	0.734	-0.090	0.165
VRFs	-0.003	0.967	-0.001	0.988	-0.084	0.187	0.181	0.016	0.066	0.295
Education	0.116	0.089	0.334	<0.001	-0.225	0.001	0.288	<0.001	-0.147	0.025
APOE	-0.157	0.017	-0.123	0.043	0.121	0.057	0.017	0.835	0.153	0.016
FW	-0.162	0.028*	-0.190	0.006*	0.226	0.002*	-0.256	0.004*	0.117	0.100
									0.223	0.001*

Note: Bold and * meant corrected by FDR, β -std, and standardized betas.

Abbreviations: FW, free water; Logical Memory-Delayed Recall; MMSE, Mini-Mental State Exam; MoCA, Montreal Cognitive Assessment; TMT-A, Trail Making Test-A; TMT-B, Trail Making Test-B; VRFs, vascular risk factor score.

allele carrier status was associated with a faster increase in FW in the A β negative group. FW was associated with global cognition, memory, and executive function in both cross-sectional and longitudinal analyses. These results may provide insights for understanding the influence of AQP4 SNPs on the glymphatic system and AD progression.

This is the first in vivo study revealing the effect of AQP4 SNPs on WM FW. FW is a diffusion imaging marker that measures the fraction of water content with unrestricted and isotropic diffusion. An elevated FW may reflect an increase in ISF (Duering et al. 2018; Zhang, Huang, et al. 2021; Zhang, Zhou, et al. 2021). Because AQP4 proteins are crucial for the CSF-ISF exchange, their structural and functional variations may alter the water permeability and change the glymphatic flow. A previous study found that mice with genetic deletion of AQP4 (AQP4 KO) had larger interstitial spaces and higher brain water content, despite a similar CSF production rate and vascular density (Gomolka et al. 2023). Furthermore, the increased interstitial space was associated with a higher water diffusivity. These results suggested that AQP4 KO could result in a reduction in glymphatic flow and lead to stagnation of fluid in the interstitial space. Although this evidence is useful for understanding the modulation of glymphatic flow and for developing potential treatment methods, no study has investigated the effect of AQP4 SNPs on glymphatic function in humans, which could be mild compared to the extreme gene knock-out approaches.

The AQP4 is encoded by a 3 kb gene located on chromosome 18. Depending on the selection of two transcription starting sites, it can be translated into AQP4-M1 or AQP4-M23 isoforms, which differ in structural characteristics and their ability to form orthogonal arrays of particles, thereby affecting the water permeability of AQP4 (Nagelhus and Ottersen 2013; Smith et al. 2014). The rs72878794 is located in the promoter region upstream of exon 0 of the AQP4 gene (Figure 2). Its polymorphism may lead to differential expression of isoforms and subsequent downstream events (Zhang, Huang, et al. 2021; Zhang, Zhou, et al. 2021; Hook-Barnard and Hinton 2007). In the cortex of AD patients, a decrease in the M1-to-M23 isoform ratio was associated with changes in the localization of AQP4 (Zeppenfeld et al. 2017), but how they exactly influence AD pathology accumulation awaits further investigation. Chandra et al. (Chandra et al. 2021) found that AQP4 SNP rs72878794 minor allele carrier status was associated with decreased Florbetapir SUVRs, and they inferred that an altered glymphatic function might mediate the association. Here, we found that the AQP4 SNP rs72878794 minor allele carrier status was associated with a slower longitudinal increase in FW. Consistent with Chandra's study, this result implies a protective role of rs72878794 minor allele carrier status.

The rs9951307 is located at the C-terminal end of AQP4, approximately 15 kb downstream of the AQP4 UGA canonical stop codon (Rainey-Smith et al. 2018), in a region that lacks known transcription factor-binding sites. Burfeind's study (Burfeind et al. 2017), using a longitudinal aging cohort, found that rs9951307 minor allele carrier status was associated with a slower cognitive decline in subjects diagnosed with AD. However, we found that the rs9951307 minor allele

TABLE 5 | Associations between baseline glymphatic imaging markers and longitudinal changes in cognitive measures in the whole group.

Independent variables	Cognitive assessment															
	MMSE			MoCA			CDR global			Logistic delayed			TMT-A		TMT-B	
	β	p		β	p		β	p		β	p		β	p	β	p
Age	0.001	0.942		-0.053	0.081		-0.004	0.142		0.068	0.210		0.313	0.007	1.713	0.001
Sex	-0.057	0.776		-0.764	0.059		0.047	0.189		-1.561	0.029		2.256	0.143	8.801	0.203
Education	0.101	0.006		0.399	<0.001		-0.014	0.031		0.493	<0.001		-0.847	0.003	-6.544	<0.001
APOE	-0.633	0.002		-0.543	0.188		0.078	0.032		-1.498	0.044		3.625	0.023	18.064	0.012
VRFs	0.026	0.815		-0.025	0.909		-0.007	0.728		0.657	0.095		0.131	0.879	-0.772	0.842
FW	-3.864	0.117		-5.756	0.258		0.655	0.142		-29.748	0.001		27.087	0.154	217.417	0.014
Time	0.572	0.005		0.326	0.293		-0.110	<0.001		-0.055	0.893		-4.268	<0.001	-1.768	0.643
FWxtime	-2.952	0.001*		-2.384	0.073		0.550	<0.001*		0.043	0.980		20.491	<0.001*	11.080	0.500

Note: Reported are estimates and *p*-values from linear mixed models with random intercepts and random slopes. The fixed effect of lymphatic marker*time was interpreted as the effect on longitudinal lymphatic change. Bold and * meant corrected by FDR.

Abbreviations: FW, free water; Logical Delayed, Logical Memory-Delayed Recall; MMSE, Mini-Mental State Exam; MoCA, Montreal Cognitive Assessment; TMT-A, Trail Making Test-A; TMT-B, Trail Making Test-B; VRFs, vascular risk factor score.

carrier status was associated with a faster increase in FW, which is detrimental, in the A β -negative group. The discrepancy may result from various reasons. Burfeind's study included subjects diagnosed with AD. Because clinically diagnosed AD was already in a late stage, complex degenerative pathologies might be involved, obscuring the effect of AQP4 SNPs. Studying non-demented populations may reduce these confounding factors and provide an understanding of early pathological mechanisms. Our finding is consistent with a study showing that rs9951307 minor allele status was associated with severe brain edema (Kleffner et al. 2008) in stroke patients. Since rs9951307 does not change the amino acid sequence, it is unlikely to affect the function of AQP4. Its association with clinical features might be due to other gene variations that are in linkage disequilibrium with rs9951307, but further experiments are needed to gain insights about the detailed mechanisms.

FW has been found sensitive to cognitive impairments. Maillard (Maillard et al. 2017) et al. found that higher baseline FW was associated with lower global cognition, memory, and executive function. Furthermore, longitudinal changes in FW were also associated with the decline of cognitive function. Several other studies also reported the relationships in community cohorts, patients with cerebral vascular diseases (Huang et al. 2022), AD continuum (Kamagata et al. 2022; Zhu et al. 2022), etc. In this study, we confirmed their associations in both cross-sectional and longitudinal analyses. However, there was no significant correlation between FW and amyloid accumulation, and we had not investigated the association between FW and tau due to a small sample size. It should be noted that ISF stagnation may influence the clearance of a wide range of metabolic wastes and poisonous proteins, and it may cause brain degeneration through other pathological mechanisms rather than amyloid accumulation. Further studies are needed to clarify the detailed mechanism.

We did not observe any associations between SNPs and PVS or ALPS. Although the three imaging markers are all related to the glymphatic system, they reflect different structural or functional properties, as discussed above. These properties are influenced by distinct pathological processes, such as arterial stiffness or venous collagenosis. As a result, the three markers may not exhibit simultaneous changes under a specific disease condition but instead display varied alteration patterns across different neurological diseases.

This study is subject to several limitations. First, we included only SNPs that are associated with AD, and thus, we cannot dismiss the potential impact of previously reported SNPs unrelated to AD on our results. Second, the sample size was relatively small for uncovering associations between genetic variations and clinical or imaging features due to the requirements for genetic data and multi-sequence imaging data. This limitation may explain the lack of significant findings regarding PVS and DTI-ALPS. Similarly, although AQP4 SNPs were associated with FW, and FW was associated with cognitive scores, we did not observe a mediation effect, possibly due to a small effect size. While ADNI is already the largest multi-center project focused on AD, a substantial portion of data has not yet been released. Future studies with larger sample sizes are necessary to validate

our findings. Third, the involvement of multiple research centers may contribute to variability in diffusion metrics. However, as the acquisition protocol of ADNI has been harmonized by a specialized imaging core and we have conducted multi-center harmonization, these differences should have been minimized. Lastly, although we used the three most widely used markers to represent glymphatic-related changes, the pathophysiological underpinnings of these markers are still undergoing validation. Caution should be exercised when interpreting the results.

5 | Conclusion

AQP4 SNPs are associated with FW accumulation, which is further associated with longitudinal cognitive decline.

6 | ADNI Consortia Information

Data used in preparation of this article were obtained from the Alzheimer's Disease Neuroimaging Initiative (ADNI) database (adni.loni.usc.edu). As such, the investigators within the ADNI contributed to the design and implementation of ADNI and/or provided data but did not participate in analysis or writing of this report. A complete listing of ADNI investigators can be found at: http://adni.loni.usc.edu/wp-content/uploads/how_to_apply/ADNI_Acknowledgement_List.pdf.

Author Contributions

Lingyun Liu and Qingze Zeng: conceptualization; methodology; writing – review and editing; data curation. Xiao Luo: conceptualization; methodology; data curation. Hui Hong: methodology; writing – review and editing. Yi Fang: conceptualization; methodology. Linyun Xie, Yao Zhang, Miao Lin, Shuyue Wang, Kaicheng Li, and Xiaocao Liu: data curation. Ruiting Zhang and Yanxing Chen: writing – review. Yunjun Yang and Peiyu Huang: conceptualization; methodology; writing – review and editing.

Acknowledgements

The data collection and sharing for this project were funded by the ADNI (National Institutes of Health Grant U01 AG024904) and DOD ADNI (Department of Defense Award No. W81XWH-12-2-0012). ADNI was funded by the NIA and the NIBIB and through generous contributions from the following: AbbVie, Alzheimer's Association; Alzheimer's Drug Discovery Foundation; Araclon Biotech; Bio Clinica Inc.; Biogen; Bristol-Myers Squibb Company; Cere Spir Inc.; Eisai Inc.; Elan Pharmaceuticals Inc.; Eli Lilly and Company; Euro Immun; F. Hoffmann-La Roche Ltd. and its affiliated company Genentech Inc.; Fujirebio; GE Healthcare; IXICO Ltd.; Janssen Alzheimer Immunotherapy Research & Development LLC; Johnson & Johnson Pharmaceutical Research & Development LLC; Lumosity; Lundbeck; Merck & Co. Inc.; MesoScale Diagnostics LLC; NeuroRx Research; Neurotrack Technologies; Novartis Pharmaceuticals Corporation; Pfizer Inc.; Piramal Imaging; Servier; Takeda Pharmaceutical Company; and Transition Therapeutics. The Canadian Institutes of Health Research is providing funds to support ADNI clinical sites in Canada. Private sector contributions are facilitated by the Foundation for the National Institutes of Health (www.fnih.org). The grantee organization is the Northern California Institute for Research and Education, and the study is coordinated by the AD Cooperative Study at the University of California, San Diego. ADNI data are disseminated by the Laboratory for Neuroimaging at the University of Southern California.

Ethics Statement

All procedures performed in studies involving human participants were under the ethical standards of the Institutional and National Research Committee and with the 1964 Helsinki declaration and its later amendments or comparable ethical standards. Written informed consent was obtained from all participants and authorized representatives, and the study partners before any protocol-specific procedures were carried out in the ADNI study. More details can be found at <http://www.adni-info.org>.

Consent

The authors have nothing to report.

Conflicts of Interest

The authors declare no conflicts of interest.

Data Availability Statement

The data that support the findings of this study are openly available in ADNI at <https://ida.loni.usc.edu/home/projectPage.jsp?project=ADNI>.

References

- Benveniste, H., H. Lee, F. Ding, et al. 2017. "Anesthesia With Dexmedetomidine and Low-Dose Isoflurane Increases Solute Transport via the Glymphatic Pathway in Rat Brain When Compared With High-Dose Isoflurane." *Anesthesiology* 127: 976–988. <https://doi.org/10.1097/ALN.0000000000001888>.
- Brown, R., H. Benveniste, S. E. Black, et al. 2018. "Understanding the Role of the Perivascular Space in Cerebral Small Vessel Disease." *Cardiovascular Research* 114: 1462–1473. <https://doi.org/10.1093/cvr/cvy113>.
- Burfeind, K. G., C. F. Murchison, S. K. Westaway, et al. 2017. "The Effects of Noncoding Aquaporin-4 Single-Nucleotide Polymorphisms on Cognition and Functional Progression of Alzheimer's Disease." *A&D Transl Res & Clin Interv* 3: 348–359. <https://doi.org/10.1016/j.trci.2017.05.001>.
- Chandra, A., C. Farrell, H. Wilson, et al. 2021. "Aquaporin-4 Polymorphisms Predict Amyloid Burden and Clinical Outcome in the Alzheimer's Disease Spectrum." *Neurobiology of Aging* 97: 1–9. <https://doi.org/10.1016/j.neurobiolaging.2020.06.007>.
- Dikmen, S. S., R. K. Heaton, I. Grant, and N. R. Temkin. 1999. "Test-Retest Reliability and Practice Effects of Expanded Halstead-Reitan Neuropsychological Test Battery." *Journal of the International Neuropsychological Society* 5: 346–356.
- Duering, M., S. Finsterwalder, E. Baykara, et al. 2018. "Free Water Determines Diffusion Alterations and Clinical Status in Cerebral Small Vessel Disease." *Alzheimers Dement* 14: 764–774. <https://doi.org/10.1016/j.jalz.2017.12.007>.
- Fang, Y., S. Dai, C. Jin, et al. 2022. "Aquaporin-4 Polymorphisms Are Associated With Cognitive Performance in Parkinson's Disease." *Frontiers in Aging Neuroscience* 13: 740491. <https://doi.org/10.3389/fnagi.2021.740491>.
- Fortin, J.-P., D. Parker, B. Tunç, et al. 2017. "Harmonization of Multi-Site Diffusion Tensor Imaging Data." *NeuroImage* 161: 149–170. <https://doi.org/10.1016/j.neuroimage.2017.08.047>.
- Gomolka, R. S., L. M. Hablitz, H. Mestre, et al. 2023. "Loss of Aquaporin-4 Results in Glymphatic System Dysfunction via Brain-Wide Interstitial Fluid Stagnation." *eLife* 12: e82232. <https://doi.org/10.7554/eLife.82232>.
- Hill, W. G., and A. Robertson. 1968. "Linkage Disequilibrium in Finite Populations." *Theoretical and Applied Genetics* 38: 226–231. <https://doi.org/10.1007/BF01245622>.

- Hong, H., L. Hong, X. Luo, et al. 2024. "The Relationship Between Amyloid Pathology, Cerebral Small Vessel Disease, Glymphatic Dysfunction, and Cognition: A Study Based on Alzheimer's Disease Continuum Participants." *Alzheimer's Research & Therapy* 16: 43. <https://doi.org/10.1186/s13195-024-01407-w>.
- Hook-Barnard, I. G., and D. M. Hinton. 2007. "Transcription Initiation by Mix and Match Elements: Flexibility for Polymerase Binding to Bacterial Promoters." *Gene Regulation and Systems Biology* 1: 275–293. <https://doi.org/10.1177/117762500700100020>.
- Hosking, L., S. Lumsden, K. Lewis, et al. 2004. "Detection of Genotyping Errors by Hardy-Weinberg Equilibrium Testing." *European Journal of Human Genetics* 12: 395–399. <https://doi.org/10.1038/sj.ejhg.5201164>.
- Huang, P., R. Zhang, Y. Jiaerken, et al. 2022. "White Matter Free Water Is a Composite Marker of Cerebral Small Vessel Degeneration." *Translational Stroke Research* 13: 56–64. <https://doi.org/10.1007/s12975-021-00899-0>.
- Huang, S., Y.-R. Zhang, Y. Guo, et al. 2024. "Glymphatic System Dysfunction Predicts Amyloid Deposition, Neurodegeneration, and Clinical Progression in Alzheimer's Disease." *Alzheimer's & Dementia* 20, no. 5: alz.13789. <https://doi.org/10.1002/alz.13789>.
- Illiff, J. J., M. Wang, Y. Liao, et al. 2012. "A Paravascular Pathway Facilitates CSF Flow Through the Brain Parenchyma and the Clearance of Interstitial Solutes, Including Amyloid β ." *Science Translational Medicine* 4: 147ra111. <https://doi.org/10.1126/scitranslmed.3003748>.
- Ishida, K., K. Yamada, R. Nishiyama, et al. 2022. "Glymphatic System Clears Extracellular Tau and Protects From Tau Aggregation and Neurodegeneration." *Journal of Experimental Medicine* 219: e20211275. <https://doi.org/10.1084/jem.20211275>.
- Kamagata, K., C. Andica, K. Takabayashi, et al. 2022. "Association of MRI Indices of Glymphatic System With Amyloid Deposition and Cognition in Mild Cognitive Impairment and Alzheimer Disease." *Neurology* 99: e2648–e2660. <https://doi.org/10.1212/WNL.0000000000201300>.
- Keshavan, A., J. Pannee, T. K. Karikari, et al. 2021. "Population-Based Blood Screening for Preclinical Alzheimer's Disease in a British Birth Cohort at Age 70." *Brain* 144: 434–449. <https://doi.org/10.1093/brain/awaa403>.
- Kleffner, I., M. Bungeroth, H. Schiffbauer, W. R. Schäbitz, E. B. Ringelstein, and G. Kuhlenbäumer. 2008. "The Role of Aquaporin-4 Polymorphisms in the Development of Brain Edema After Middle Cerebral Artery Occlusion." *Stroke* 39: 1333–1335. <https://doi.org/10.1161/STROKEAHA.107.500785>.
- Li, K., S. Wang, X. Luo, et al. 2023. "Associations of Alzheimer's Disease Pathology and Small Vessel Disease With Cerebral White Matter Degeneration: A Tract-Based MR Diffusion Imaging Study." *Journal of Magnetic Resonance Imaging* 60, no. 1: 268–278. <https://doi.org/10.1002/jmri.29022>.
- Maillard, P., G. F. Mitchell, J. J. Himali, et al. 2017. "Aortic Stiffness, Increased White Matter Free Water, and Altered Microstructural Integrity: A Continuum of Injury." *Stroke* 48: 1567–1573. <https://doi.org/10.1161/STROKEAHA.116.016321>.
- Mestre, H., L. M. Hablitz, A. L. Xavier, et al. 2018. "Aquaporin-4-Dependent Glymphatic Solute Transport in the Rodent Brain." 7: e40070. <https://doi.org/10.7554/eLife.40070>.
- Nagelhus, E. A., and O. P. Ottersen. 2013. "Physiological Roles of Aquaporin-4 in Brain." *Physiological Reviews* 93: 1543–1562. <https://doi.org/10.1152/physrev.00011.2013>.
- Nedergaard, M. 2013. "Garbage Truck of the Brain." *Science* 340: 1529–1530. <https://doi.org/10.1126/science.1240514>.
- Nedergaard, M., and S. A. Goldman. 2020. "Glymphatic Failure as a Final Common Pathway to Dementia." *Science* 370: 50–56. <https://doi.org/10.1126/science.abb8739>.
- Oh, E. S., P. B. Rosenberg, G. B. Rattinger, E. A. Stuart, C. G. Lyketsos, and J. M. S. Leoutsakos. 2021. "Psychotropic Medication and Cognitive, Functional, and Neuropsychiatric Outcomes in Alzheimer's Disease (AD)." *Journal of the American Geriatrics Society* 69: 955–963. <https://doi.org/10.1111/jgs.16970>.
- Pasternak, O., N. Sochen, Y. Gur, N. Intrator, and Y. Assaf. 2009. "Free Water Elimination and Mapping From Diffusion MRI." *Magnetic Resonance in Medicine* 62: 717–730. <https://doi.org/10.1002/mrm.22055>.
- Perosa, V., J. Oltmer, L. P. Munting, et al. 2022. "Perivascular Space Dilation Is Associated With Vascular Amyloid- β Accumulation in the Overlying Cortex." *Acta Neuropathologica* 143: 331–348. <https://doi.org/10.1007/s00401-021-02393-1>.
- Purcell, S., B. Neale, K. Todd-Brown, et al. 2007. "PLINK: A Tool Set for Whole-Genome Association and Population-Based Linkage Analyses." *American Journal of Human Genetics* 81: 559–575. <https://doi.org/10.1086/519795>.
- Rainey-Smith, S. R., G. N. Mazzucchelli, V. L. Villemagne, et al. 2018. "Genetic Variation in Aquaporin-4 Moderates the Relationship Between Sleep and Brain A β -Amyloid Burden." *Translational Psychiatry* 8: 47. <https://doi.org/10.1038/s41398-018-0094-x>.
- Rasmussen, M. K., H. Mestre, and M. Nedergaard. 2018. "The Glymphatic Pathway in Neurological Disorders." *Lancet Neurology* 17: 1016–1024. [https://doi.org/10.1016/S1474-4422\(18\)30318-1](https://doi.org/10.1016/S1474-4422(18)30318-1).
- Royse, S. K., D. S. Minhas, B. J. Lopresti, et al. 2021. "Validation of Amyloid PET Positivity Thresholds in Centiloids: A Multisite PET Study Approach." *Alzheimer's Research & Therapy* 13: 99. <https://doi.org/10.1186/s13195-021-00836-1>.
- Saadoun, S., M. C. Papadopoulos, H. Watanabe, D. Yan, G. T. Manley, and A. S. Verkman. 2005. "Involvement of Aquaporin-4 in Astroglial Cell Migration and Glial Scar Formation." *Journal of Cell Science* 118: 5691–5698. <https://doi.org/10.1242/jcs.02680>.
- Smith, A. J., B. J. Jin, J. Ratelade, and A. S. Verkman. 2014. "Aggregation State Determines the Localization and Function of M1- and M23-Aquaporin-4 in Astrocytes." *Journal of Cell Biology* 204: 559–573. <https://doi.org/10.1083/jcb.201308118>.
- Tabangin, M. E., J. G. Woo, and L. J. Martin. 2009. "The Effect of Minor Allele Frequency on the Likelihood of Obtaining False Positives." *BMC Proceedings* 3, no. Suppl 7: S41. <https://doi.org/10.1186/1753-6561-3-S7-S41>.
- Taoka, T., Y. Masutani, H. Kawai, et al. 2017. "Evaluation of Glymphatic System Activity With the Diffusion MR Technique: Diffusion Tensor Image Analysis Along the Perivascular Space (DTI-ALPS) in Alzheimer's Disease Cases." *Japanese Journal of Radiology* 35: 172–178. <https://doi.org/10.1007/s11604-017-0617-z>.
- Tedeschi Dauar, M., T. A. Pascoal, J. Therriault, et al. 2023. "Dynamic Amyloid and Metabolic Signatures of Delayed Recall Performance Within the Clinical Spectrum of Alzheimer's Disease." *Brain Sciences* 13: 232. <https://doi.org/10.3390/brainsci13020232>.
- Tiwari, S., V. Atluri, A. Kaushik, A. Yndart, and M. Nair. 2019. "Alzheimer's Disease: Pathogenesis, Diagnostics, and Therapeutics." 14: 5541–5554. <https://doi.org/10.2147/IJN.S200490>.
- Tsang, J., J. F. Fullard, S. G. Giakoumaki, et al. 2015. "The Relationship Between Dopamine Receptor D1 and Cognitive Performance." *NPJ Schizophrenia* 1: 14002. <https://doi.org/10.1038/npjscz.2014.2>.
- Verkman, A. S. 2012. "Aquaporins in Clinical Medicine." *Annual Review of Medicine* 63: 303–316. <https://doi.org/10.1146/annurev-med-043010-193843>.
- Vittorini, M. G., A. Sahin, A. Trojan, et al. 2024. "The Glymphatic System in Migraine and Other Headaches." *Journal of Headache and Pain* 25: 34. <https://doi.org/10.1186/s10194-024-01741-2>.
- Zeng, Q., K. Li, X. Luo, et al. 2022. "The Association of Enlarged Perivascular Space With Microglia-Related Inflammation and

Alzheimer's Pathology in Cognitively Normal Elderly." *Neurobiology of Disease* 170: 105755. <https://doi.org/10.1016/j.nbd.2022.105755>.

Zeppenfeld, D. M., M. Simon, J. D. Haswell, et al. 2017. "Association of Perivascular Localization of Aquaporin-4 With Cognition and Alzheimer Disease in Aging Brains." *JAMA Neurology* 74: 91. <https://doi.org/10.1001/jamaneurol.2016.4370>.

Zhang, R., P. Huang, Y. Jiaerken, et al. 2021a. "Venous Disruption Affects White Matter Integrity Through Increased Interstitial Fluid in Cerebral Small Vessel Disease." *Journal of Cerebral Blood Flow and Metabolism* 41: 157–165. <https://doi.org/10.1177/0271678X20904840>.

Zhang, W., Y. Zhou, J. Wang, et al. 2021b. "Glymphatic Clearance Function in Patients With Cerebral Small Vessel Disease." *NeuroImage* 238: 118257. <https://doi.org/10.1016/j.neuroimage.2021.118257>.

Zhu, Y.-C., C. Dufouil, B. Mazoyer, et al. 2011. "Frequency and Location of Dilated Virchow-Robin Spaces in Elderly People: A Population-Based 3D MR Imaging Study." *AJNR. American Journal of Neuroradiology* 32: 709–713. <https://doi.org/10.3174/ajnr.A2366>.

Zhu, Z., Q. Zeng, R. Zhan, et al. 2022. "White Matter Free Water Outperforms Cerebral Small Vessel Disease Total Score in Predicting Cognitive Decline in Persons With Mild Cognitive Impairment." *JAD* 86: 741–751. <https://doi.org/10.3233/JAD-215541>.

Supporting Information

Additional supporting information can be found online in the Supporting Information section.